

# In Situ Solvothermal Synthesis and Characterization of Transparent Epoxy/TiO<sub>2</sub> Nanocomposites

Haiying Zhang,<sup>1</sup> Rongrong Qi,<sup>1</sup> Mingkang Tong,<sup>1</sup> Yaozhen Su,<sup>2</sup> Mark Huang<sup>3</sup>

<sup>1</sup>School of Chemistry and Chemical Engineering, Shanghai Jiao Tong University, Shanghai 200240, China

<sup>2</sup>School of Aeronautics and Astronautics, Shanghai Jiao Tong University, Shanghai 200240, China

<sup>3</sup>Institute of Microelectronics, A\*STAR, Singapore 117685, Singapore

Received 21 October 2010; accepted 18 April 2011

DOI 10.1002/app.34699

Published online 6 January 2012 in Wiley Online Library (wileyonlinelibrary.com).

**ABSTRACT:** A solvothermal process was developed to *in situ* prepare epoxy (EP)/TiO<sub>2</sub> hybrid precursors. The chemical structure of samples was confirmed by X-ray and Fourier transformed infrared spectroscopy. Field emission scanning electron microscope micrographs of cured EP/TiO<sub>2</sub> hybrid composites showed that well-dispersed TiO<sub>2</sub> nanoparticles were successfully *in situ* formed in epoxy matrix through the solvothermal process. The thermogravimetric analysis, DSC, and gel content measurements showed that EP/TiO<sub>2</sub> hybrid precursors were fully cured with the glass transition temperature decreasing gradually. The effect of TiO<sub>2</sub> contents on optical and surface proper-

ties was investigated in detail. The results indicated that epoxy/TiO<sub>2</sub> nanocomposites exhibited excellent UV shielding effect and high visible light transparency. The contact angle of EP/TiO<sub>2</sub> nanocomposites, when the content of silane-coupling agent (KH560) was 5 g and the content of tetrabutyl titanate (TBT) was 3 g, can reach as high as 101°, which was 36° higher than that of pure EP, representing for the increase of hydrophobicity. © 2012 Wiley Periodicals, Inc. *J Appl Polym Sci* 125: 1152–1160, 2012

**Key words:** epoxy resin; TiO<sub>2</sub> nanoparticles; *in situ* solvothermal process

## INTRODUCTION

Over the past decade, the preparation and characterization of organic–inorganic hybrid materials or polymer nanocomposites have received widespread attention because of their unique properties.<sup>1–6</sup> The improvement in the properties of the hybrids compared with the pure polymers is mainly attributed to the unique phase morphology and the interfacial properties, thus they could be widely used in various areas such as coatings, plastics, rubbers, sealants, and fibers and so on.<sup>7–10</sup>

In recent years, a range of metal-oxide particles have been used as inorganic components to be dispersed in the polymer matrix to prepare organic–inorganic hybrid materials.<sup>11–13</sup> The mainstream of these technologies is to widely incorporate nanometer-sized particles into the polymer matrix for further studies.<sup>14–17</sup> Compared with the conventional microparticles, nanoparticles were found to possess special advantages such as better adhesion to the matrix and improved modifying effect with a lower content of fillers.<sup>18,19</sup>

However, there exists a challenge for nanoparticles to be homogeneously dispersed into the polymer

matrix without agglomeration arising from nanosized dimension and extremely high specific surface areas. To avoid the agglomeration of nanoparticles, two methods have been studied to achieve the uniform dispersion. One approach is to pretreat the surfaces of nanoparticles with silane-coupling agents to improve the compatibility between the matrix and the nanoparticles. Another method is to prepare nanoparticles by *in situ* synthesis of sol–gel precursors. The sol–gel process involves a series of hydrolysis and subsequent condensation reactions of metal alkoxide precursors.<sup>20,21</sup> Beyond these approaches, some types of coupling agents are simultaneously added to improve the surface compatibility through chemical bonding and restrict macroscopic phase separations.<sup>22</sup>

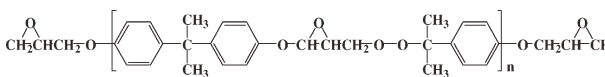
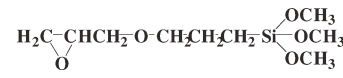
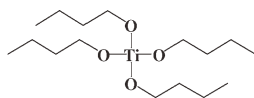
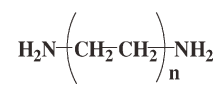
Epoxy resin is one of the most important thermosetting polymer materials in industry owing to its excellent thermal stability, strong adhesion strength, and outstanding mechanical, electrical properties and so on. Epoxy nanocomposites are often prepared using a great variety of methods such as hot pressing, sol–gel processing, molecular composite generation, and ultrafine particles dispersion.<sup>23–26</sup> Among these methods, the sol–gel process is a widely used technique. Epoxy (EP)/SiO<sub>2</sub> nanocomposites,<sup>20</sup> EP/TiO<sub>2</sub> composites etc.<sup>10,22,27–30</sup> have been mainly prepared by the sol–gel process. However, a large amount of solvent such as THF is used in this process, and in most cases the samples are cast into films for further characterization. At the same time, degassing of solvents is normally needed for the composites in sheet form after the sol–gel process.

Correspondence to: R. Qi (rrqi@sjtu.edu.cn).

Contract grant sponsor: The National Science Foundation of China; contract grant number: 21173145.

Contract grant sponsor: Shanghai Leading Academic Discipline Project; contract grant number: B202.

TABLE I  
Structures of the Materials Employed

Starting materials	Chemical structures
E-51	
3-Glycidoxypropyltrimethoxysilane (KH560)	
Tetrabutyl titanate (TBT)	
Curing agent 5784	

Solvothermal synthesis is a newly developed method to prepare nanoparticles or nanocomposites.<sup>31,32</sup> Compared with the conventional synthesis routes, the solvothermal synthesis possesses some distinct characteristics such as very high self-generated pressure inside the sealed reaction vessel (autogenous pressure), controllability of volatile products, milder conditions, and facile process without calcination at high temperature.

It is worth mentioning that the epoxy resin is easy to degrade upon exposure to the UV-light during the manufacturing process, storage, and application. The conventional methods to improve the anti-aging properties include either the addition of antioxidants<sup>33</sup> or organic UV absorbing agents<sup>34,35</sup> or light stabilizers. However, these methodologies have the inherent disadvantages because organic UV absorbing agents can be destroyed by UV lights in some cases and thus deteriorate their chemical stability and photo-stability in long run. In recent years, inorganic particles such as nano-ZnO and nano-TiO<sub>2</sub> have widely been used to improve the anti-aging properties of epoxy resins owing to their strong UV absorbance and other characteristics. For example, TiO<sub>2</sub> possesses strong photocatalytic properties and excellent ultraviolet absorption properties which are effective for aging-resistant properties of polymers.<sup>36</sup> Apart from UV-resistance, TiO<sub>2</sub> also improved the mechanical, thermal, optical, electronic, and surface properties of the polymer/TiO<sub>2</sub> composites.<sup>27,37,38</sup> Another research interest is to prepare low surface-energy epoxy resin materials through surface modification.<sup>39-42</sup>

This article focuses on synthesis of transparent EP/TiO<sub>2</sub> nanohybrids. Specifically, EP/TiO<sub>2</sub> hybrid precursors were prepared by *in situ* solvothermal process and further cured to obtain EP/TiO<sub>2</sub> nanohybrids. Tetrabutyl titanate (TBT) was employed as precursors to prepare TiO<sub>2</sub> nanoparticles in liquid epoxy monomer as reaction medium. KH560 was added as a coupling agent to improve interfacial interaction between

the epoxy matrix and *in situ*-formed TiO<sub>2</sub> nanoparticles and simultaneously as a diluent to reduce viscosity of epoxy matrix. After completion of *in situ* synthesis, the transparency, UV absorbance, morphology, and surface properties of EP/TiO<sub>2</sub> hybrid nanocomposites were further characterized.

## EXPERIMENTAL

### Materials

Epoxy resin (E-51) (diglycidyl ether of bisphenol A) was purchased from Tianyuan Group Shanghai Resin Factory Co. (Shanghai, China). Curing agent 5784 is a modified long-chain aliphatic primary amine (colorless and transparent viscous liquid), purchased from Tianyuan Group Resin Factory Co. (Shanghai, China). TBT (chemical reagent grade) was ordered from Sinopharm Chemical Reagent Co. (Shanghai, China). Dibutyltin dilaurate (DBTDL) was purchased from Rongrong Chemical Co. (Shanghai, China). 3-Glycidoxypropyltrimethoxysilane (KH560) (Yaohua Chemical Co., Shanghai, China) was used as a coupling agent. Mold release agent F-303 I was purchased from HD Chemical Co. (Shanghai, China). Hydrochloric acid and acetone (both analytical reagent grade) were supplied by Lingfeng Chemical Solvent Co. (Shanghai, China). Ethanol was ordered from Changshu chemical Co., Changshu, China. All the solvents were used as received.

### Solvothermal synthesis of TiO<sub>2</sub>-containing epoxy precursor

The hydrolysis and condensation of TBT were performed in a sealed vessel. The starting materials for *in situ* solvothermal synthesis of TiO<sub>2</sub>-containing epoxy precursors were highlighted in Table I, whereas the recipes for the synthesis are summarized in Table II. It should be noted that the epoxy resin needed preheating to 80°C to reduce its viscosity. The mixing of KH560,

**TABLE II**  
The Recipes for Synthesis of TiO<sub>2</sub>/Epoxy Nanocomposites

Sample code	EP (g)	KH560 (g)	TBT (g)	HCl (g)	Ethanol/(g)
P-EP	30	0	0	0	0
ET0	30	5	0	0.3	2.5
ET1	30	5	1	0.3	2.5
ET2	30	5	2	0.3	2.5
ET3	30	5	3	0.3	2.5
ET4	30	5	4	0.3	2.5
ET5	30	5	5	0.3	2.5

TBT, ethanol, hydrochloric acid, and preheated epoxy monomer were carried out in an autoclave. After stirring for 10 min, the mixture became homogenous. Then the sealed vessel was put into a constant temperature oven. After a certain time, the products were taken away from the vessel. The final precursor was obtained after removal of residual small molecules under vacuum at 60°C to a constant weight.

#### *In situ* polymerization of EP/TiO<sub>2</sub> hybrids

The mixture of EP/TiO<sub>2</sub> hybrid precursor and a stoichiometric amount of curing agent 5784 (50 g/100 g of epoxy resin) were blended and degassed in vacuum at 50°C for about 30 min. The resulting mixture was then poured into a metal mold sprayed with mold release agent. All samples were cured at 80°C for 2 h and post cured at 100°C for 3 h in an oven.

#### Characterization of EP/TiO<sub>2</sub> nanocomposites

##### X-ray diffractory

The crystal behavior of different samples was analyzed by XRD-6000 Diffraction Analyzer (Shimadzu UV-2450, Kyoto, Japan).

##### Fourier transformed infrared (FTIR) spectroscopy

The FTIR spectra of samples were performed on Spectrum 100 (Perkin-Elmer, Massachusetts, MN) between 450 cm<sup>-1</sup> and 4000 cm<sup>-1</sup>.

##### Gel content

The gel content test of the cured samples was conducted in Soxhlet apparatus (DaFeng Glass Ware Factory, Shanghai, China) using acetone as solvent at 100°C for 24 h extraction and then samples were dried at 60°C in an oven to a constant weight; and the weight loss was measured to calculate the gel content. The calculation formula is as follows:

$$\text{Gel content}(\%) = m_2/m_1 \times 100\%$$

where  $m_2$ : The sample weight after extraction;  $m_1$ : The sample weight before extraction.

#### Curing kinetics

Differential scanning calorimetry (DSC) was carried out using a TA instrument (Q2000, TA Instruments, New Castle, Delaware) at a heating rate of 10°C/min, under nitrogen flux.

#### Thermal stability

Thermogravimetric analysis (TGA) was performed using a TA instrument (Q5000, TA Instruments, New Castle, Delaware) at a heating rate of 20°C/min under N<sub>2</sub> atmosphere, in the range between the room temperature and 700°C.

#### Surface property

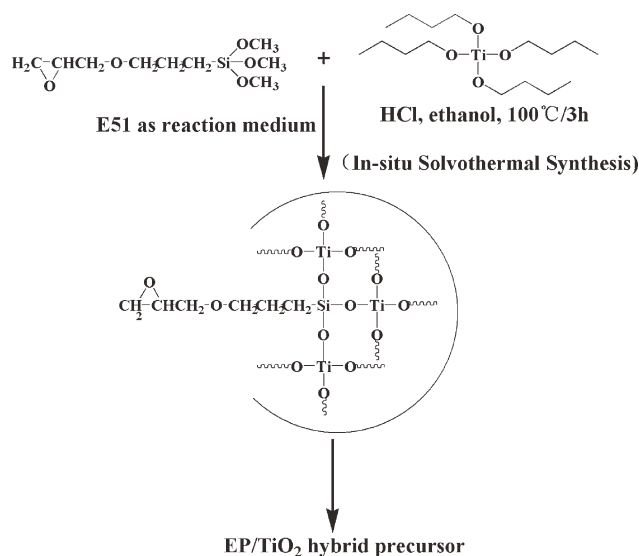
Contact angle measurement was performed with a contact angle system OCA20 (Data Physics Instruments GmbH, Stuttgart, Germany) equipped with a video camera. Analysis was made at room temperature by means of the sessile drop technique. The volume of every drop was 3.5 μL. Three to five times measurements were performed on every sample and the values were averaged. The measuring liquid was double distilled water ( $\gamma = 72.88 \text{ mN m}^{-1}$ ).

#### Optical property

UV-Vis spectra were measured on a spectrophotometer (Shimadzu UV-2450, Kyoto, Japan) in the range between 300 nm and 700 nm.

#### Morphology

The morphology and dispersion of TiO<sub>2</sub> nanoparticles in the epoxy matrix was examined using field emission scanning electron microscope (FE-SEM) (JSM-7401F, JEOL, Tokyo, Japan).



**Scheme 1** Synthesis of EP/TiO<sub>2</sub> precursor.





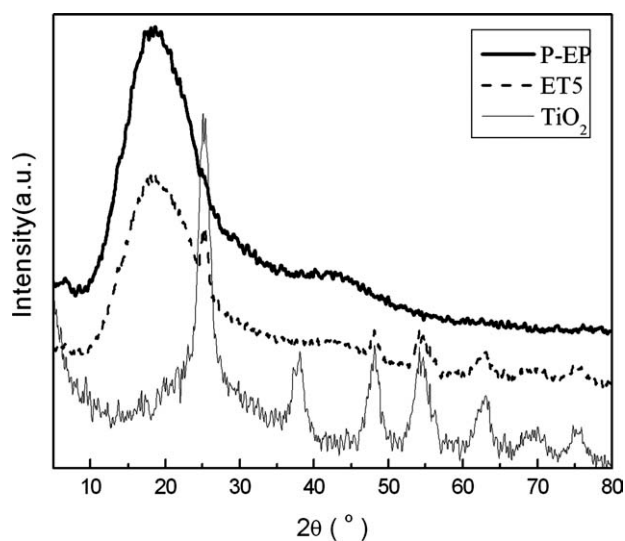


**Figure 1** X-ray diffraction patterns of three samples.

curing agent 5786 upon heat treatment to fabricate EP/TiO<sub>2</sub> nanocomposites, as illustrated in Scheme 2.

To prove the successful synthesis of TiO<sub>2</sub> in the epoxy matrix and EP/TiO<sub>2</sub> hybrid precursors, the XRD patterns for pure TiO<sub>2</sub>, pure EP, and ET5 are given in Figure 1. It can be seen that pure EP displayed only a very broad hump peak with its diffraction angle ( $2\theta$ ) ranging between 10° and 30°, indicating the amorphous phase of EP. From the diffraction curve of TiO<sub>2</sub> nanoparticles synthesized in the same condition as ET5, it can be found that the peaks were very sharp and the strong peaks at  $2\theta = 25.3^\circ$  corresponded to the (101) crystal plane of anatase phase of TiO<sub>2</sub>. And also other crystal planes such as, (004), (200), (211), (204) corresponded to the standard diffraction patterns of face-centered tetragonal anatase titanium dioxide (JPCDS NO.21-1272),<sup>43-45</sup> which confirmed successful formation of pure anatase phase in given solvothermal reaction condition. According to the calculation of Scherrer equation using the (101) peak, the average crystalline size of the anatase phase TiO<sub>2</sub> was around 4 nm. From the XRD patterns of ET5, it can be clearly seen that the broad hump peak of EP matrix covered the main two crystal planes (101) and (004) of anatase phase TiO<sub>2</sub>, but other crystal planes could be observed, which confirmed successful *in situ* solvothermal synthesis of EP/TiO<sub>2</sub> nanocomposites.

To further prove the successful preparation of EP/TiO<sub>2</sub> precursors, the FTIR spectra of (a) P-TiO<sub>2</sub>; (b) ET0; (c) ET3 was measured. In Figure 2(a), a broad absorption peak between 500 cm<sup>-1</sup> and 800 cm<sup>-1</sup> belonged to Ti—O—Ti absorption bands, indicating the presence of TiO<sub>2</sub>.<sup>46</sup> Figure 2(b) showed the FTIR spectra of ET0 without TBT, and the peak at 916 cm<sup>-1</sup> was attributed to epoxide group absorption<sup>46</sup> while the peak at around 1120 cm<sup>-1</sup> was assigned to the Si—O—Si asymmetric stretching,<sup>47</sup> indicating the

hydrolysis of KH560 in solvothermal conditions. While in Figure 2(c), the absorption band at around 916 cm<sup>-1</sup> confirmed the existence of epoxide group of epoxy matrix. There was also the broad absorption at lower wave number region. Especially 1109 cm<sup>-1</sup> was assigned to the Si—O—Si and Si—O—Ti.<sup>47</sup> The shift of the Si—O band toward lower wave number has been observed by introducing metallic oxides<sup>48</sup> due to the formation of Si—O—M (M is second metal atom) hetero-linkages. In this article, the shift of the 1120 cm<sup>-1</sup> band to 1109 cm<sup>-1</sup> band with the increase of Ti content may thus indicate a gradual increase of Si—O—Ti population in the epoxy matrix from the comparison of Figure 2(b,c).

To obtain EP/TiO<sub>2</sub> nanocomposites, TBT components was first hydrolyzed in HCl in the epoxy resin monomer matrix followed by curing reaction of epoxy resin as curing agent 5768 was added into EP/TiO<sub>2</sub> precursors. The viscous epoxy resin can effectively prevent the aggregation of TiO<sub>2</sub> particles. After curing reaction of epoxy resin system, the as-formed TiO<sub>2</sub> particles remained in the original state, which was further confirmed using FE-SEM. Figure 3(c) showed the FE-SEM micrographs of EP/TiO<sub>2</sub> nanocomposites for sample ET3. The particle size ranging from 20 nm to 200 nm was uniformly embedded in the epoxy matrix without any significant agglomerations. And the cured pure epoxy resin had a smooth and flat surface morphology as shown in Figure 3(a) after cross-linking of epoxy resin. As the TBT content increased, more TiO<sub>2</sub> particles were observed in EP matrix. The results proved that EP/TiO<sub>2</sub> nanocomposites were successfully synthesized through *in situ* solvothermal process.

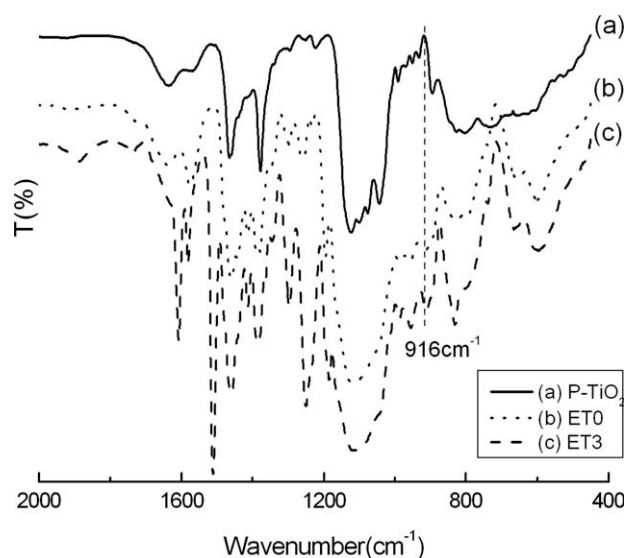


**Figure 2** The FTIR spectra of (a) P-TiO<sub>2</sub>; (b) ET0; and (c) ET3 samples.

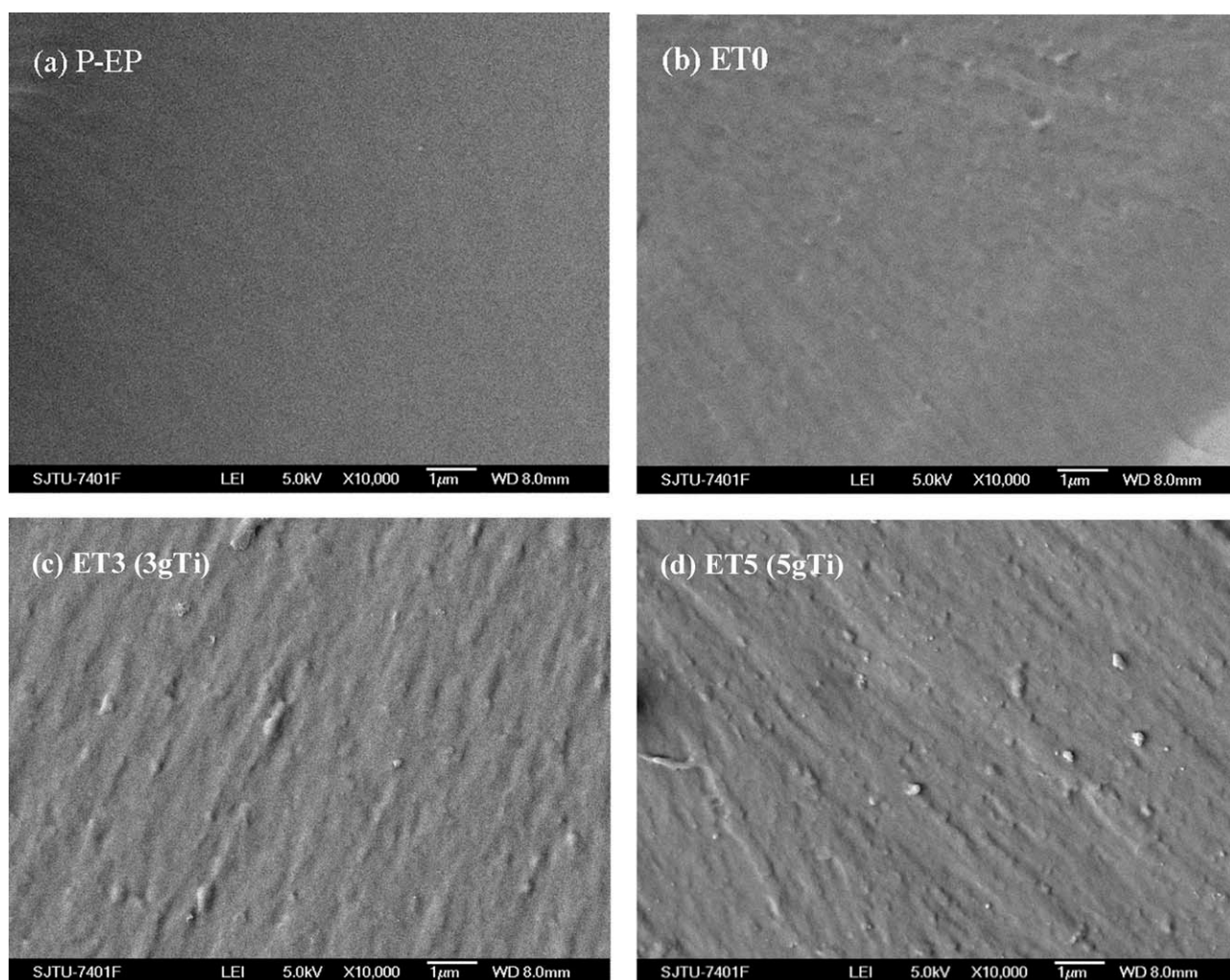


**Figure 3** FE-SEM micrographs of (a) P-EP; (b) ET0; (c) ET3; and (d) ET5 after curing.

### Effect of TiO<sub>2</sub> nanoparticles on curing reaction of EP

To find out whether the formation of TiO<sub>2</sub> nanoparticles affected the curing process of epoxy matrix, DSC analysis was carried out on the samples of EP/TiO<sub>2</sub> hybrid precursors of different TiO<sub>2</sub> contents. Figure 4 showed the dynamic DSC thermograms of pure EP and its nanocomposites with different TiO<sub>2</sub> contents. In this figure, the exothermal peak of EP/TiO<sub>2</sub> hybrids slightly shifted to lower temperature as compared with the exothermal peak temperature of pure epoxy resin, which suggested that TBT most likely acted as a catalyst to accelerate the curing process of epoxy resin. The reason was probably that TiO<sub>2</sub> nanoparticles in the EP matrix could absorb partial epoxy molecules by van der Waals force to form interfacial layer because of high specific surface area and high surface energy of TiO<sub>2</sub> nanoparticles. The epoxy molecules outside interfacial layer could be easily cured with curing agents while those inside interfacial layer were difficult to react with curing

agents because the strong interaction between TiO<sub>2</sub> nanoparticles and epoxy molecules made the curing agent hard to enter into interfacial layer to react with epoxy, which meant that with respect to the epoxy molecules outside interfacial layer, there was excessive amount of curing agents and so the exothermal peak temperature dropped.<sup>49</sup>

### Effect of TiO<sub>2</sub> and silane KH560 on thermal properties of EP/SiO<sub>2</sub> nanocomposites

The thermal properties including the degree of curing, the glass transition temperature ( $T_g$ ), the thermal stability of cured EP/TiO<sub>2</sub> nanocomposites, were characterized using DSC and TGA. This article focused on the impact of *in situ* formed TiO<sub>2</sub> and silane-coupling agent KH560 on glass transition temperature ( $T_g$ ) and maximum degradation temperature ( $T_d$ ) of EP/TiO<sub>2</sub> nanocomposites, as given in Table III. Pure epoxy resin (P-EP) was used as control with  $T_g$  value of 65.2°C. It is interesting to find

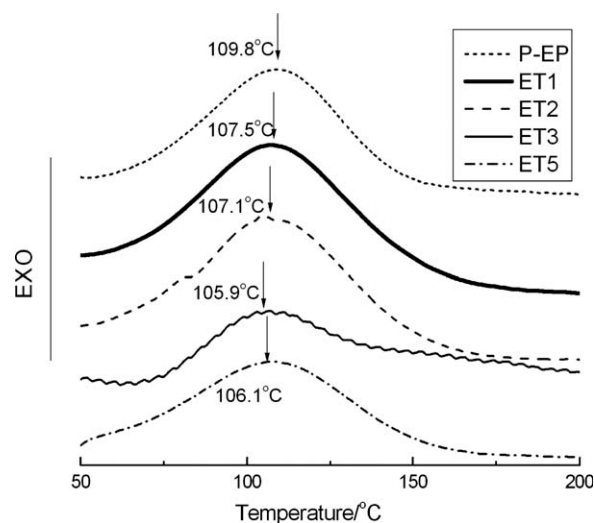


**Figure 4** DSC thermograms of EP/TiO<sub>2</sub> hybrid precursors of different TiO<sub>2</sub> contents.

that the addition of silane-coupling agent KH560 can reduce the  $T_g$  value (60.2°C) of cured EP. Further incorporation of TiO<sub>2</sub> nanoparticles can remarkably lower the  $T_g$  (42.8°C) of EP/TiO<sub>2</sub> nanocomposites. This probably resulted from the phenomenon that the interaction between epoxy resin molecular chain and the surface of TiO<sub>2</sub> nanoparticles hindered the epoxy molecular chain entanglement, which made the epoxy molecular chain around TiO<sub>2</sub> nanoparticles easy to move, thereby reducing the glass transition temperature of the entire EP system.<sup>50</sup>

From Table III, it can be also seen that the gel contents of all samples were all very high (>95%), indicating that in any case, the curing process had formed a nearly fully cross-linked networks. Moreover, the maximum degradation temperature ( $T_d$ ) of EP/TiO<sub>2</sub> nanocomposites was around 370°C, which meant that degradation of epoxy resin backbone was not largely affected by the existence of the inorganic phases TiO<sub>2</sub>.

### Optical properties of EP/TiO<sub>2</sub> nanocomposites

The transmittance in the range of visible wavelength as well as the digital appearance of the pure cured EP and cured EP/TiO<sub>2</sub> nanocomposites are showed in Figure 5. The transmittance of pure EP and EP/TiO<sub>2</sub> hybrids was above 80% in visible light spectra and almost con-

**TABLE III**  
Effect of *In Situ* Formed TiO<sub>2</sub> on Thermal Behaviors of EP/TiO<sub>2</sub> Nanocomposites

Sample code	KH560 (g)	TBT (g)	Gel content (%)	Glass transition temperature ( $T_g$ , °C)	Maximum degradation temperature ( $T_d$ , °C)
P-EP	0	0	97.2	65.2	371.5
ET0	5	0	98.2	60.2	365.9
ET3	5	3	99.3	42.8	366.6

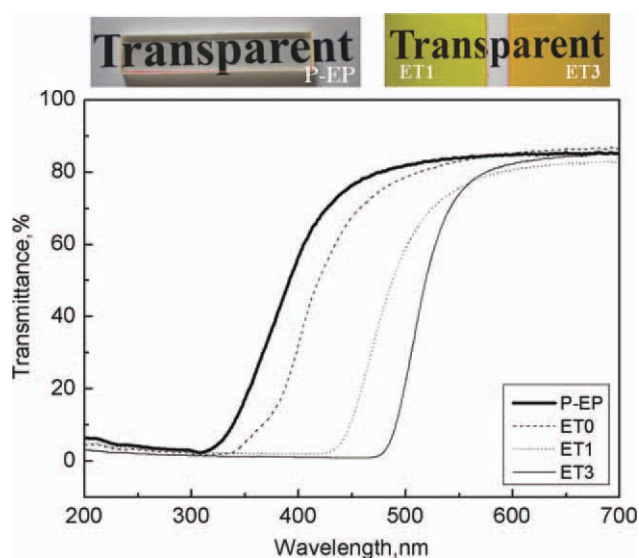


**Figure 5** The transparency and appearance of P-EP and EP/TiO<sub>2</sub> nanocomposites. [Color figure can be viewed in the online issue, which is available at wileyonlinelibrary.com.]

stant with varied concentrations of TBT and KH560. Both the P-EP and the cured EP/TiO<sub>2</sub> nanocomposites containing different TBT contents were fully transparent to visible light which could be attributed to a uniform distribution of titania nanoparticles. The high transparency of EP/TiO<sub>2</sub> nanocomposites is also attributed to the phenomenon that the addition of the silane-coupling agent KH560 can provide a strong bonding between the organic and inorganic phases and at the same time improve the compatibility between epoxy matrix and TiO<sub>2</sub>, thereby leading to the formation of transparent hybrids.

The P-EP was colorless while the other samples (ET1 and ET3) were yellow in appearance as shown in Figure 5(Top). This is probably attributed to the complexation of TBT hydrolysis products after solvothermal process and only through the high-temperature calcinations the complexation could be destroyed to form white TiO<sub>2</sub> powders. And the phenomenon was the same with those in other published articles.<sup>47</sup>

Long-wave ultraviolet (320–400 nm) shows the strongest penetrability into human skins among the range of UV wavelength, thereby directly results to skin aging and skin disease. To this end, there is a great demand for developing special sunscreen creams and sun-shading health materials.<sup>51</sup> The transmittance and absorbance of EP/TiO<sub>2</sub> nanocomposites in the range of ultraviolet wavelength are shown in Figure 6. It is found that the absorbance intensity of UV rays increased with the increasing TBT contents, which can also be reflected in the transmittance curves [Fig. 6(a)]. The transmittance of sample ET2 and ET3 nearly reached zero at the range of 300–400 nm, indicating



that the TiO<sub>2</sub> nanoparticles in epoxy matrix possessed a strong UV absorbance, which was also confirmed in other papers.<sup>39</sup> Moreover, the effect of shielding UV light was strengthened with the TBT content increasing from 1 g to 3 g. The characteristic absorption of TiO<sub>2</sub> nanoparticles<sup>52</sup> in Figure 6 further confirmed the formation of TiO<sub>2</sub> nanoparticles in epoxy matrix through *in situ* solvothermal process.

### Surface properties EP/TiO<sub>2</sub> nanocomposites

Epoxy composites have wide applications such as coatings and structural materials. Some need the certain anti-fouling ability to avoid dust or pollutant deposition. So it is indispensable to investigate the surface properties of epoxy composites. In this study, the contact angle measurements of the obtained EP/TiO<sub>2</sub> nanocomposites were performed. Figure 7 gave the effect of TBT contents on contact angles of different samples. It was found that the contact angle of pure epoxy resin with water was 65°, showing a hydrophilic surface. The contact angle increased when only adding silane-coupling agent KH560 and then dropped when the TBT content was 1 g or 2 g, and

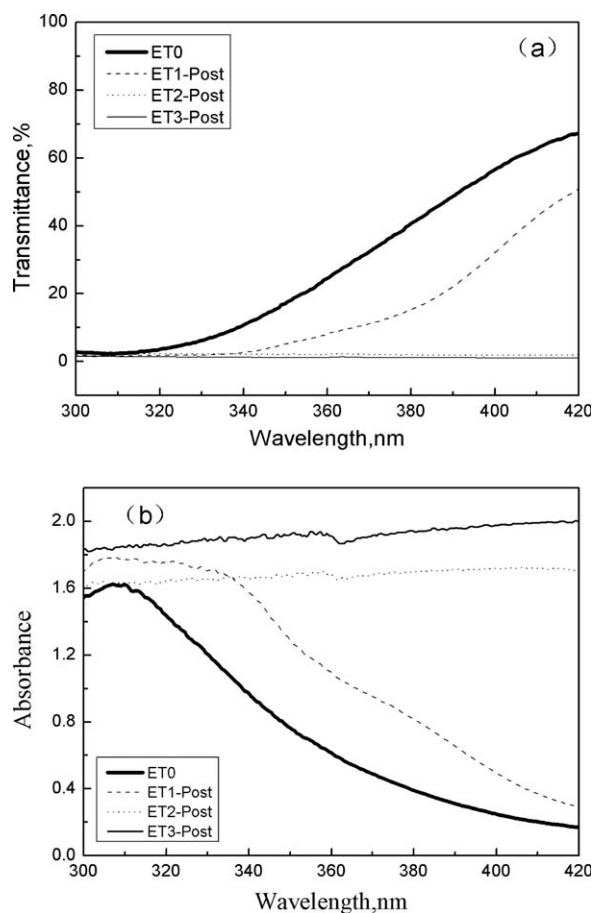


**Figure 6** Effect of TBT concentrations on UV absorption of the pure EP and EP/TiO<sub>2</sub> hybrids: (a) Transmittance; (b) Absorbance.

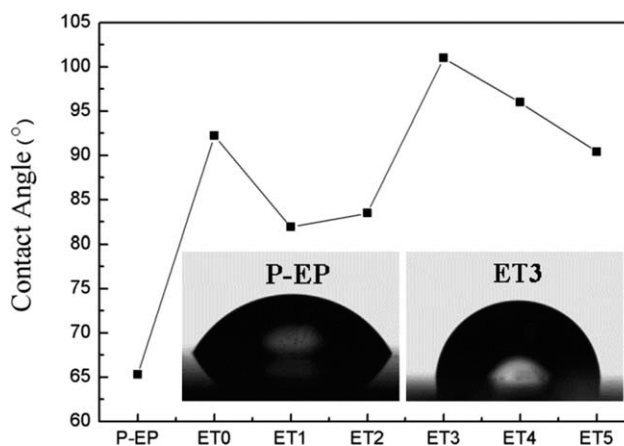


**Figure 7** Effect of TBT content on contact angles with water as medium.

then the contact angle rose again to as high as 101° when the TBT content reached 3 g, and after that declined again as the TBT kept increasing.

In this experiment, there were three factors to affect the contact angles. First, large amounts of nonpolar methylene groups ( $-\text{CH}_2-$ ) on the chain of KH560 exhibited excellent hydrophobicity toward polar water molecules which induced an increase of contact angles. Second, the surface of TiO<sub>2</sub> nanoparticles formed in the EP matrix by solvothermal process possess a lot of hydroxyl group ( $-\text{OH}$ ), which could interact with water molecules to form hydrogen bonds, thereby inducing an improved hydrophilicity and decrease of contact angles. Third, the formation of nano-TiO<sub>2</sub> made the matrix surface rougher and uneven just like the surface structures of lotus leaves and therefore certain surface roughness could lead to the improvement of hydrophobicity and the increase of contact angles. The hybrid ET0 showed a steep increase of contact angle (CA) by approximately 92° compared with pure epoxy resin, indicating that the great transformation of the surface from hydrophilicity to hydrophobicity. This can be attributed to the first factor above that the existence of a large amount of methylene groups ( $-\text{CH}_2-$ ) on the chain of KH560 increased the contact angle. When a small quantity of TBT (1 g or 2 g) was added into epoxy matrix with certain content of KH560, the contact angle was dropped by about 10° compared with ET0. That is because the second factor played a more important role in affecting the contact angles. When the content of TBT was 3 g, the contact angle reached the maximum value of 101°, which was probably attributed to more formation of nano-TiO<sub>2</sub> made the EP matrix surface rougher and uneven and therefore led to the improvement of hydrophobicity and increase of contact angles, as shown in FE-SEM micrographs in Figure 3. With the continuing increase of TBT content, more Ti-OH groups were formed and the contact angles declined with an increase of hydrophilicity.



## CONCLUSIONS

In general, the solvothermal process was introduced to *in situ* synthesis of EP/TiO<sub>2</sub> hybrid precursors first, and then as-formed EP/TiO<sub>2</sub> hybrid precursors reacted with curing agents to transparent EP/TiO<sub>2</sub> nanocomposites. Furthermore, the morphology and properties of EP/TiO<sub>2</sub> nanocomposites were discussed in detail. The important results are summarized as follows:

1. The well-dispersed TiO<sub>2</sub> nanoparticles were successfully *in situ* formed in epoxy matrix. Moreover, TBT might act as a catalyst to accelerate the dynamic curing process of EP/TiO<sub>2</sub> system.
2. EP/TiO<sub>2</sub> nanocomposites were fully cured with high gel contents (>95%) and  $T_g$  decreased gradually with the increase of TBT content.
3. EP/TiO<sub>2</sub> hybrid materials exhibit high transparency and excellent UV light shielding effect.
4. EP/TiO<sub>2</sub> nanocomposites with high contact angle (101°) have been obtained when the content of KH560 was 5 g and the content of TBT was 3 g, which was 36° higher than that of pure EP, indicating the transformation from hydrophilic surface to hydrophobic surface.

## References

1. Chiang, P. C.; Whang, W. T. *Polymer* 2003, 44, 2249.
2. Lee, L. H.; Chen, W. C. *Polymer* 2005, 46, 2163.
3. Xu, H. Y.; Kuo, S. W.; Lee, J. S. *Polymer* 2002, 43, 5117.
4. Matejka, L.; Dukh, O.; Kamišová, H. *Polymer* 2004, 45, 3267.
5. Liu, Y. L.; Su, Y. H.; Lai, J. Y. *Polymer* 2004, 45, 6831.
6. Jeng, R. J.; Chang, C. C.; Chen, C. P. *Polymer* 2003, 44, 143.
7. Zhang, M. Q.; Rong, M. Z.; Zheng, Y. X.; Zeng, H. M.; Friedrich, K. *Polymer* 2001, 42, 3301.
8. Singh, R. P.; Zhang, M.; Chan, D. *J Mater Sci* 2002, 37, 781.
9. Xie, X. L.; Liu, Q. X.; Li, R. K. Y.; Zhang, Q. X.; Yu, Z. Z.; Mai, Y. W. *Polymer* 2004, 45, 6665.
10. Liu, C. L.; Cui, Z. C.; Guan, C.; Guan, J. Q.; Yang, B.; Shen, J. C. *Macromol Mater Eng* 2003, 288, 717.
11. Hajji, P.; David, L.; Gerard, J. F.; Pascault, J. P.; Vigier, G. *J Polym Sci Part B: Polym Phys* 1999, 37, 3172.
12. Schmidt, H.; Jonschker, G.; Goedicke, S.; Menning, M. *J Sol-Gel Sci Technol* 2000, 19, 39.
13. Cho, J. D.; Ju, H. T.; Hong, J. W. *J Polym Sci Part A: Polym Chem* 2005, 43, 658.
14. Xian, G. J.; Walter, R.; Hauptert, F. *J Synth Lubr* 2005, 21, 269.
15. Wetzel, B.; Hauptert, F.; Friedrich, K.; Zhang, M. Q.; Rong, M. Z. *Polym Eng Sci* 1919, 2002, 42.
16. Xing, X. S.; Li, R. K. Y. *Wear* 2004, 256, 21.
17. Xian, G.; Walter, R.; Hauptert, F. *Materialwiss Werkst* 2004, 35, 670.
18. Ajayan, P. M.; Schadler, L. S.; Braun, P. V.; *Nanocomposite Science and Technology*; Wiley: New York, 2004.
19. Schwartz, C. J.; Bahadur, S. *Wear* 2000, 237, 261.
20. Amerio, E.; Sangermano, M.; Malucelli, G.; Priola, A.; Voit, B. *Polymer* 2005, 46, 11241.
21. Bandyopadhyay, A.; Bhowmick, A. R.; De Sarkor, M. *J Appl Polym Sci* 2004, 93, 2579.
22. Sangermano, M.; Malucelli, G.; Amerio, E.; Bongiovanni, R.; Di Gianni, A.; Voit, B.; Rizza, G. *Macromol Mater Eng* 2006, 291, 517.
23. Novotny, V. *Liq Surf* 1987, 24, 361.
24. Kojima, Y.; Usuki, A. *J Mater Res* 1993, 8, 1185.
25. Saegusa, T. *Pure Appl Chem* 1965, 1995, 67.
26. Vaia, R. A.; Jandt, K. D.; Kramer, E. J.; Giannelis, E. P. *Macromolecules* 1995, 28, 8080.
27. Chang, C. C.; Chen, W. C. *J Polym Sci Part A: Polym Chem* 2001, 39, 3419.
28. Yeh, J. M.; Wenig, C. J.; Huang, K. Y.; Huang, H. Y.; Yu, Y. H. *J Appl Polym Sci* 2004, 94, 400.
29. Xiong, M.; You, B.; Zhou, S.; Wu, L. *Polymer* 2004, 45, 2967.
30. Xiong, M.; Zhou, S.; Wu, L.; Wang, B.; Yang, L. *Polymer* 2004, 45, 8127.
31. Qian, X. F.; Yin, J.; Guo, X. X.; Yang, Y. F.; Zhu, Z.; Lu, J. *J Mater Sci Lett* 2000, 19, 2235.
32. Qian, X. F.; Yin, J.; Yang, Y. F.; Lu, Q. H.; Zhu, Z. K.; Lu, J. *J Appl Polym Sci* 2001, 82, 2744.
33. Geogre, G. A.; Sacher, R. E.; Sprouse, J. F. *J Appl Polym Sci* 1977, 21, 2241.
34. Hu, M. L.; Chen, Y. K.; Chen, L. C.; Sano, M. *J Nutr Biochem* 1995, 6, 504.
35. Allen, J. M.; Gossett, C. J.; Allen, S. K. *J Photochem Photobiol B: Biol* 1996, 32, 33.
36. Fujishima, A.; Rao, T. N.; Tryk, D. A. *J Photochem Photobiol C* 2000, 1, 1.
37. Liu, J.; Siddiqui, J. A.; Ottenbrite, R. M. *Polym Adv Technol* 2001, 12, 285.
38. Cossigneau, T.; Fendler, J. H.; Johnson, S.; Mallouk, T. E. *Adv Mater* 2000, 12, 1363.
39. Tang, J. J.; Su, C. H. *J Jiangsu Univ Sci Technol. Nat Sci Ed* 2009, 23, 125.
40. Huang, L.; Xiao, T. P. F. *Bull Chin Ceram Soc* 2008, 27, 1067.
41. Chen, M. L.; Qu, Y. Y.; Yang, L.; Gao, H. *Sci China Ser B Chem* 2008, 51, 848.
42. Li, C.; Zhang, G. Z. *New Build Mater* 2008, 35, 81.
43. Sharma, S. D.; Sing, D.; Saini, K. K.; Kant, K.; Sharma, V.; Jain, S. C.; Sharma, C. P. *Appl Catal A Gen* 2006, 314, 140.
44. Sreemany, M.; Sen, S. *Mater Chem Phys* 2004, 83, 169.
45. Luca, D.; Mardare, D.; Iacomi, F.; Teodorescu, C. M. *Appl Surf Sci* 2006, 252, 6122.
46. Huang, K. S.; Nien, Y. H.; Chen, J. S.; Shieh, T. R.; Chen, J. W. *Polym Compos* 2006, 27, 195.
47. Lu, S. R.; Zhang, H. L.; Zhao, C. X.; Wang, X.-Y. *J Macromol Sci Part A: Pure Appl Chem* 2005, 42, 1691.
48. Sohn, J. R.; Jang, H. J. *J Catal* 1991, 132, 563.
49. Zhang, H.; Zhang, Z.; Friedrich, K.; Eger, C. *Acta Mater* 2006, 54, 1833.
50. Ash, B. J.; Schadler, L. S.; Siegel, R. W. *Mater Lett* 2002, 55, 83.
51. Li, G. H.; Li, C. Z.; Zhou, Y. H. *Chem World* 2000, 2, 59.
52. Xu, B.; Zhong, M. Q.; Sun, L.; Xiong, S. F.; Xu, L. X. *Polym Mater Sci Eng* 2007, 23, 137.